

Article

Exploring the Correlation between Block Vitality and Block Environment Based on Multisource Big Data: Taking Wuhan City as an Example

Yunzi Yang¹, Yuanyuan Ma¹ and Hongzan Jiao^{1,2,*}

¹ Department of Urban Planning, School of Urban Design, Wuhan University, Wuhan 430072, China; yangyunzi@whu.edu.cn (Y.Y.); yuanyuanma@whu.edu.cn (Y.M.)

² Engineering Research Center of Human Settlements and Environment of Hubei Province, Wuhan 430072, China

* Correspondence: Jiaohongzan@whu.edu.cn; Tel.: +86-27-6877-3062

Abstract: Block is the basic unit for studying the urban activities of residents, and block vitality is the concrete expression of urban dynamics at the block level. The quality of the block's residential environment is a crucial medium to satisfy the residents' pursuit of high-quality life; good block quality is essential for fostering the block vitality and further enhancing the overall vitality of the city. This study used the distribution density of cellular signaling data to quantify block vitality and constructed a block environment index system covering four dimensions—block accessibility, block function, block development degree, and human perception of block environment—innovatively introducing the elements of block environment from the human perspective. Considering the variability of block vitality between workdays and weekends, and between downtown and suburban blocks, this study used a geographically weighted regression model to show the mechanism of the spatial and temporal influence of indicators on block vitality, as well as to suggest how to enhance block vitality at different times of the day based on the influence mechanism. This study was conducted in Wuhan, China. The findings suggest that block vitality exhibited significant spatial and temporal heterogeneity. A high-vitality block can be created by enhancing the block's accessibility, increasing the degree of block construction, and enriching the functional density and mix of functions in the block. A pleasantly green environment with a moderate degree of openness exerted a significant impact on promoting human activity and enhancing block vitality. The creation of high-vitality blocks should also consider the differences in the impact of various elements on block vitality between weekend and workday. For example, amid the surge in travel demand for education venues on weekends, enhancing the accessibility of blocks can significantly increase the vitality of blocks on weekends. We can truly realize the people-oriented approach to build a livable and high-vitality city by adapting to local conditions and time.

Keywords: block vitality; cellular signaling data; environmental perception; dynamic features; geographically weighted regression



Citation: Yang, Y.; Ma, Y.; Jiao, H. Exploring the Correlation between Block Vitality and Block Environment Based on Multisource Big Data: Taking Wuhan City as an Example. *Land* **2021**, *10*, 984. <https://doi.org/10.3390/land10090984>

Academic Editor: Fabrizio Battisti

Received: 3 August 2021

Accepted: 16 September 2021

Published: 17 September 2021

Publisher's Note: MDPI stays neutral with regard to jurisdictional claims in published maps and institutional affiliations.



Copyright: © 2021 by the authors. Licensee MDPI, Basel, Switzerland. This article is an open access article distributed under the terms and conditions of the Creative Commons Attribution (CC BY) license (<https://creativecommons.org/licenses/by/4.0/>).

1. Introduction

Jane Jacobs [1] first proposed the concept of urban vitality and used it to indicate the intensity of human activities in urban space. Later studies used this concept primarily to measure the richness of people's activities in the space and the perception of an excellent urban spatial environment. Urban vitality plays a vital role in fulfilling people's needs for a high-quality life and augmenting the overall spatial quality of cities [2,3]. Typically, blocks are areas surrounded by roads and are the fundamental building blocks of the urban fabric. From the standpoint of human behavior, a block is a shared space created by the spatial interaction of residents' behavior [4]. Urban activities and their interaction with spatial entities reflect block vitality, where spatial entities refer to geographic spaces that

support people's activities, including stores and parks [5,6]. Block vitality is a part of urban vitality. Block vitality exerts a positive impact on the health of residents, public safety of the city, and socioeconomic development [7–9]. The single function and sociality of blocks have declined people's willingness to engage in spatial interaction activities in recent years, contradicting the residents' gradually increasing demand for livability. Lately, block vitality has garnered widespread attention as a critical component of urban vitality.

As early as when urban vitality was first proposed, studies discussed the factors influencing urban vitality. Most traditional studies on urban vitality used questionnaires and field interviews to qualitatively investigate the factors and mechanisms influencing vitality and suggest ways to enhance urban vitality [3,10,11]. For example, studies proposed that the higher the building density, the narrower the neighborhood form, and the more intricate the urban function, the higher the urban vitality [12–14]. Previous studies laid the foundation with strong operability; however, these studies had limitations such as the lack of data support, limited research scope, and that the degree of influence of each element cannot be measured quantitatively [15]. With the progress of Internet technology, various open-source big data have been extensively used in academic research. These big data have the advantages of large data volume and easy access, providing robust data support to realize quantitative research on urban vitality.

Traditional quantitative studies of urban vitality mostly used small restaurant business distribution density [16,17] and nighttime lighting data [18–20] as vitality measures to measure static vitality, leading to a lack of research on the difference in vitality between workdays and weekends. However, various aspects of human activity, such as willingness to go out, activity choices, and places to travel, differ markedly between workdays and weekends [21,22]. Thus, urban vitality characterized by the intensity of human activities in the city also exhibits significant differences. Hence, it is necessary and meaningful to consider the difference in vitality between workdays and weekends in the research system. From the different attributes of urban vitality, the environmental influencing factors of urban vitality are primarily divided into two categories—social environment and physical environment [23,24]. While the social environment denotes economic elements, historical and cultural elements, and other sociological attributes, the physical environment denotes the elements of the physical space. In the research of the influence mechanism of urban vitality, three aspects of urban function, urban accessibility, and the degree of urban construction among the elements of the physical environment are used extensively [5,25–27]. Traditional research on urban function is typically measured using land-use type data, which is valid but still has disadvantages such as large scope and slow update [5]. Notably, people are the source of urban vitality and the subject of perception of the urban environment, and their perception of the external environment significantly influences their behavior. However, human perception of the environment has not been included in the research mechanism of environmental impact on vitality.

In recent years, cellular signaling data have been applied to measure regional vitality [28–30], which can truly and reliably reflect human behavior and better represent the spatial and temporal dynamics of human activities compared with traditional data of restaurant enterprises and luminous remote-sensing data. Based on the abovementioned advantages, the cellular signaling data can contribute to the study of the dynamic change characteristics of vitality on workdays and weekends and illustrate the overall vitality intensity more comprehensively [31,32]. With the availability of open-source data, the measurement of two aspects of urban function—urban function density, which can also be called land-use intensity, and urban-function-mixing degree meaning the intensity of mixed land use—has changed. The POI data are used as the most fine-grained data of urban land use to assess the function density of cities, compensating for the drawbacks of large scope and slow update of land-use type data [33,34]. In addition, the calculation of the function-mixing degree has evolved from the traditional calculation of the area and proportion of each type of land in the region to the calculation of the spatial entropy of POI; this calculation reflects a more representative degree of mixing [35,36]. People are a vital

source and component of urban vitality; however, the existing literature lacks research on how people's perception of the physical environment affects urban vitality. Some studies have attempted to explore the impact of street greening on human travel behavior. They have considered the approach of extracting vegetation indices from remote-sensing image data, which differ markedly from the greening situation shown by human eyes [37]. With the rapid advancement of multisource geospatial data, researchers have access to a large number of publicly available geotagged images [38]. The viewpoint of these streetscape images can more intuitively reflect residents' actual perceptions of their surroundings, providing the feasibility of introducing the perception of human eye vision into the influencing factors of block vitality on a large scale [39].

Previous research on urban vitality has focused on developed countries in Europe and the United States, and the exploration of the relationship between urban vitality and urban environment in China has important implications for developing countries [40]. With the development of open-source data in China, scholars have studied the relationship between block vitality and block environment in major cities such as Beijing, Shanghai, and Shenzhen [20,25,41]. The existing inquiry on the relationship between urban vitality and environment in China suffers from the shortcomings of small research scope (only some streets are studied) and failure to consider spatial heterogeneity and temporal heterogeneity [2,41,42]. This study expanded the scope of the study based on the previous work and considered the lack of vitality comparison between workdays and weekends and the lack of human eye perception in vitality research in existing studies. This study used cellular signaling data distribution density to measure block vitality and constructed four level indicators—"block development intensity", which measures the horizontal and vertical development of block land, "block function", which indicates the use of block land, "block accessibility", which is a measure of how easy it is to get around the block, and block environment perception—innovatively introducing human perception of the environment into the discussion of the correlation with block vitality. In addition, geographically weighted regression models (GWR) were used to analyze the impact of each indicator element on vitality during workdays versus weekends. The remaining components of this study are as follows: Section 2 introduces the background of the study area, the source, and preprocessing of the study data; Section 3 introduces the research methods, including the construction of the index system, image segmentation method, and the GWR; Section 4 details the research results; Sections 5 and 6 discuss the research results and analyze the strengths and weaknesses of the study.

2. Study Area and Data

2.1. Study Area

Wuhan (113°41'–115°05' E, 22°29'–31°58' N) is the capital city of Hubei Province and the central city of Central China. It is located in the eastern part of the Jiangnan Plain and the middle reaches of the Yangtze River where the Yangtze River, the third-largest river in the world, and its largest tributary, the Han River, converge in the city. Wuhan's water area accounts for a quarter of the total area of Wuhan city. With 166 lakes of all sizes, Wuhan is also known as "the city of a hundred lakes" [43].

We used the main urban area delineated in the Wuhan Master Plan 2010–2020 as the study area. The main urban area of Wuhan is dominated by the area within the Third Ring Road, including the local extension of Zhuankou, Miaoshan, and Wugang areas. It is linked by the Yangtze and Han rivers and the east–west mountain system, creating a relatively independent and complete urban system of Hankou, Wuchang, and Hanyang, with a total area of 678 km² (Figure 1).

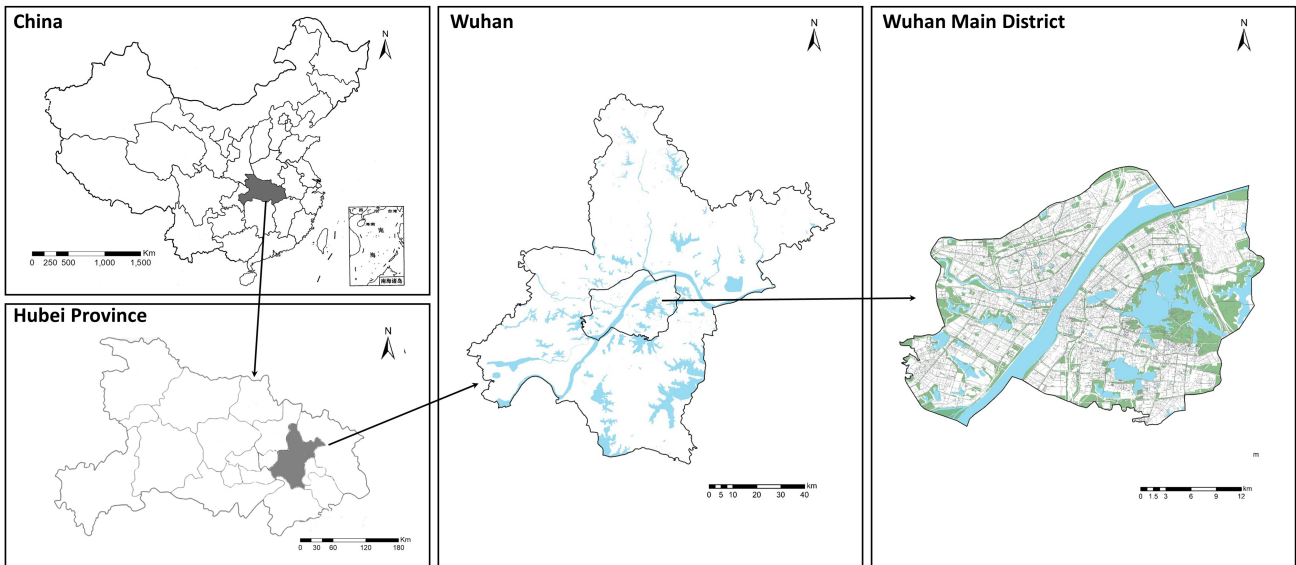


Figure 1. Wuhan city and main urban area location.

2.2. Data Sources and Preprocessing

2.2.1. Basic Data

The basic data included urban block data, urban road network data, urban public transportation data, and urban building data. Traffic analysis zone (TAZ) is used to define blocks. TAZs belong to the urban micro-medium level, and each TAZ has as similar characteristics as possible in terms of population density and land use. Thus, using TAZ data for block-level research has significant advantages. The TAZ data this study used are delineated based on the travel volume and road conditions in Wuhan in 2018. Owing to the northern boundary of the main urban area isolating part of the complete traffic zone, the study area near Tianxingzhou was marginally adjusted; Figure 2 shows the before-and-after comparison. We used 2395 TAZs with cellular signaling data within the study area, with an average area of 0.217 km², and TAZs without cellular signaling data were not included in the study area [5].

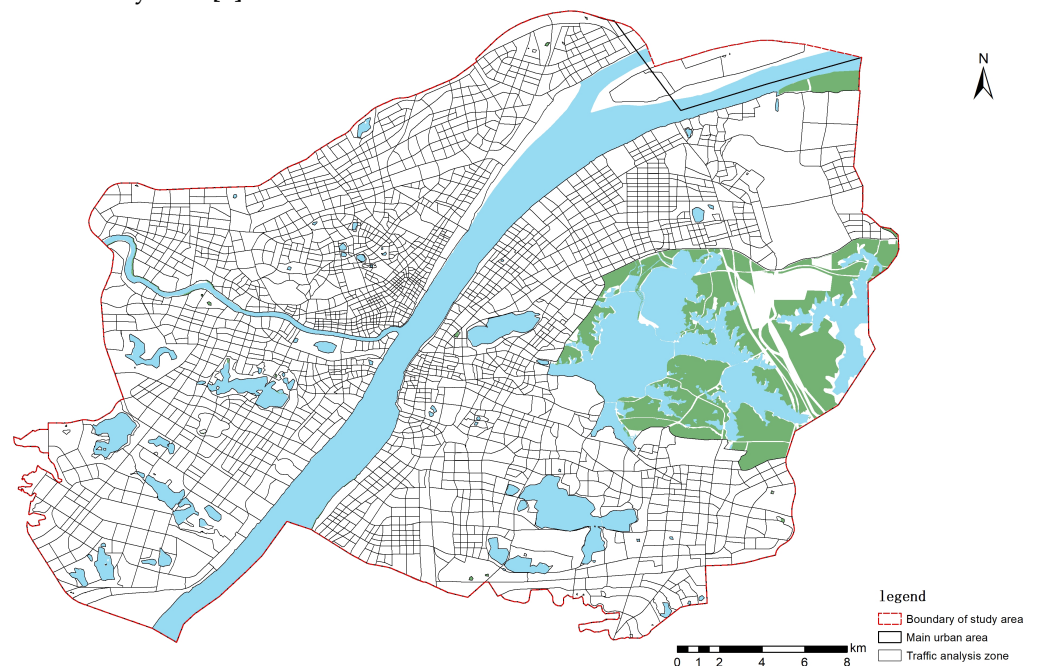


Figure 2. Comparison of main urban area scope and study area.

The urban road network data, urban public transport data, and urban building data of 2018 were obtained from the OpenStreetMap platform [44] (Figure 3). The road network data included seven levels of urban expressways, highways, national and provincial roads, county roads, township and village roads, and other roads. The urban public transportation data included information on the names and distribution locations of public transportation stations and rail transit stations within the study area. The urban building data contained basic attributes such as building height and floor area.

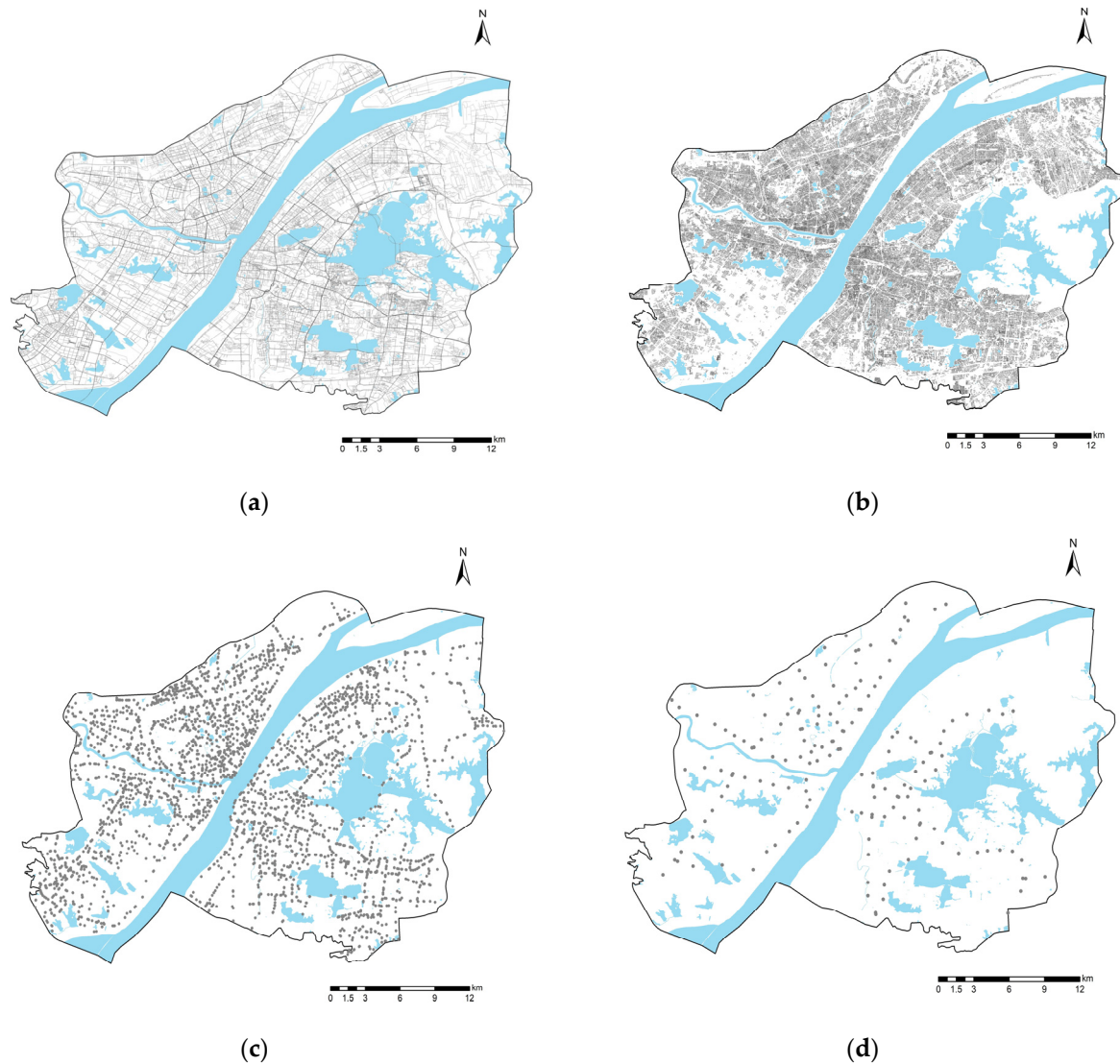


Figure 3. Basic data. (a) Road network data; (b) building data; (c) public transportation station data; (d) subway station data.

2.2.2. Cellular Signaling Data Preprocessing

It is well established that cellular signaling data can be used effectively to study human behavior [45–47]. The cellular signaling data used in this study were collected by a large mobile operator in Wuhan, whose subscribers account for 67% of all cell phone users, and the cell phone usage data it collects is highly universal and representative, reflecting the travel behavior of most people [45]. Cellular signaling data were collected by mobile operators from 5 March 2018 to 11 March 2018 and contained 5 working days and 2 rest days, which can fully reflect a cycle of human activity. This paper attempts to explore the relationship between block vitality and block environment in daily situations, and thus the time period chosen for the study is universal in that it does not include holidays and other major events with extremely variable pedestrian flow. A total of 150,704,053 communication

records were obtained from 21,995 base stations in the main urban area of Wuhan; Figure 4 shows the locations of the base stations in the main urban area. Only time information and coordinate information were extracted from each communication record, and no sensitive information was included.

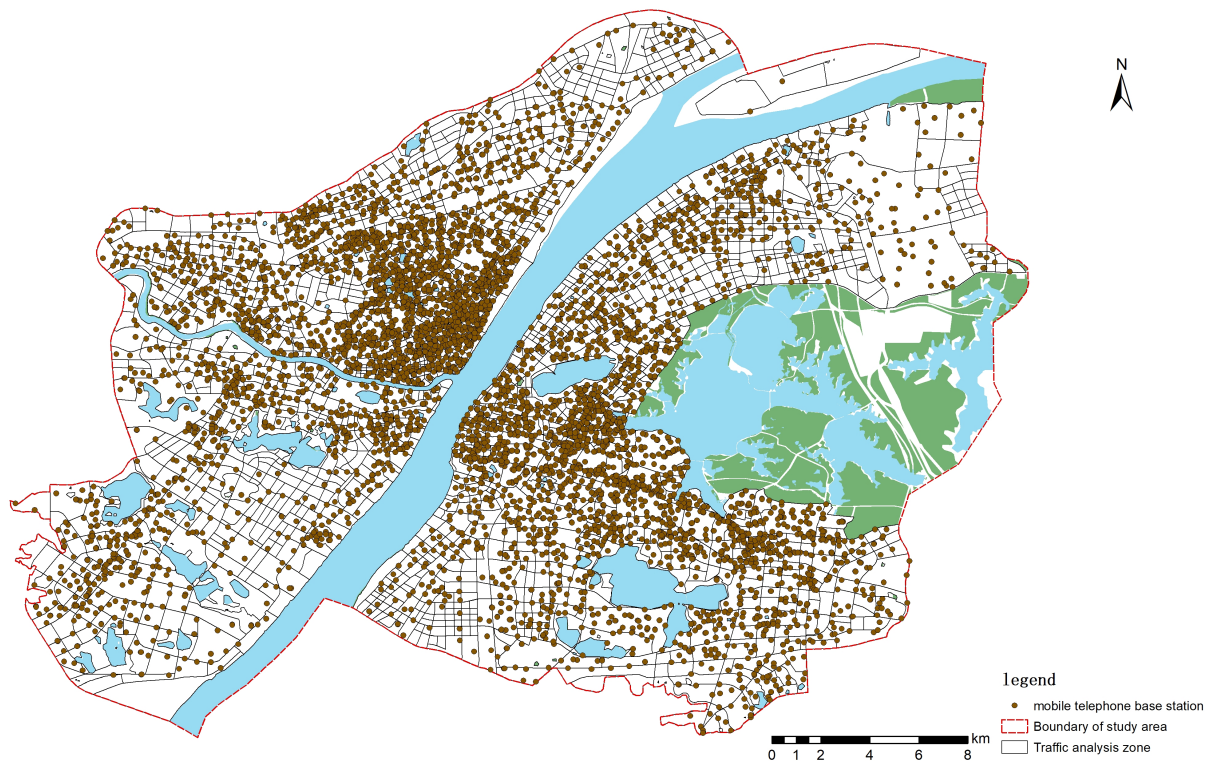


Figure 4. Base station location distribution.

2.2.3. Extraction and Preprocessing of Streetscape Images

In recent years, an increasing number of street-view images have been used for urban research applications [48]. Baidu Maps Street View has a higher collection frequency and a wider collection range in China than other providers. The Baidu Maps software, developed in 2005 by Baidu.com in Beijing, China, started releasing street maps in 2013 [49], which are available for users to browse along with an application programming interface (API) to download. The road network data within the study area were sampled at 300 m intervals, and point data with latitude and longitude coordinates were generated. We retrieved street-view images at each point location via the Baidu Maps API and automatically obtained location-specific street-view images in May 2021 through the following URL: <http://quanjing.baidu.com/apipickup/> (accessed on 12 May 2021).

A total of 95,988 points were identified, of which 5762 points did not have street pictures; thus, 90,226 sampling points were finally identified. To more accurately reflect the scenery viewed by human eyes' vision, four pictures of 0°, 90°, 180°, and 270° directions were used for each sampling point, and the combined results of the four pictures were used to reflect the street scenery of the same point. Finally, 360,904 images with an image resolution of 1024 × 512 were collected. Figure 5 shows the street-view images schematically.

2.2.4. POI Data Preprocessing

The POI data for Wuhan in 2018 were obtained from the Baidu Map by administrative region and time. We combined similar categories into 13 categories according to the official categories given, and classification is presented in Table 1. A total of 79,758 POIs within the scope were retained, and the percentage of POIs in various categories (Figure 6) and the specific spatial distribution (Figure 7) are as follows.



Figure 5. Example of street-view image.

Table 1. POI reclassification.

POI Classification in This Paper	POI Classification in Baidu Map
Accommodation Service Facilities	Accommodation Service, Commercial House
Government Agency	Governmental Organization and Social Group
Medical Service Facilities	Medical Service
Recreational Facilities	Recreational Service
Sports Facilities	Sports and Recreation
Living Service Facilities	Daily Life Service, Auto Service, Auto Repair
Cultural Facilities	Science/Culture and Education Service, Training Institutions
Financial Service Facilities	Finance and Insurance Service, Enterprises
Transportation Facilities	Transportation Service, Road Furniture, Place Name and Address, Pass Facilities
Shopping Service Facilities	Shopping
Parks and Squares	Parks and Squares
Scenic Spots	Tourist Attraction
Catering Facilities	Food and Beverage

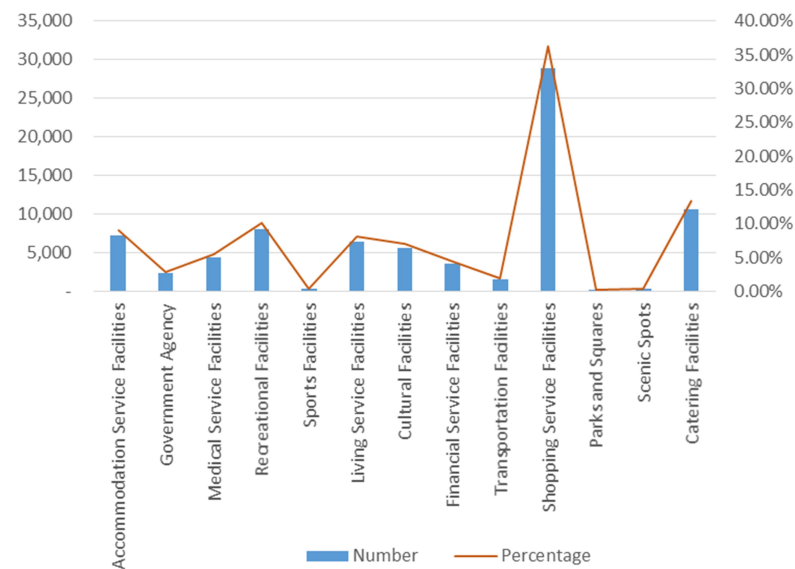


Figure 6. Percentage of POIs in each category.

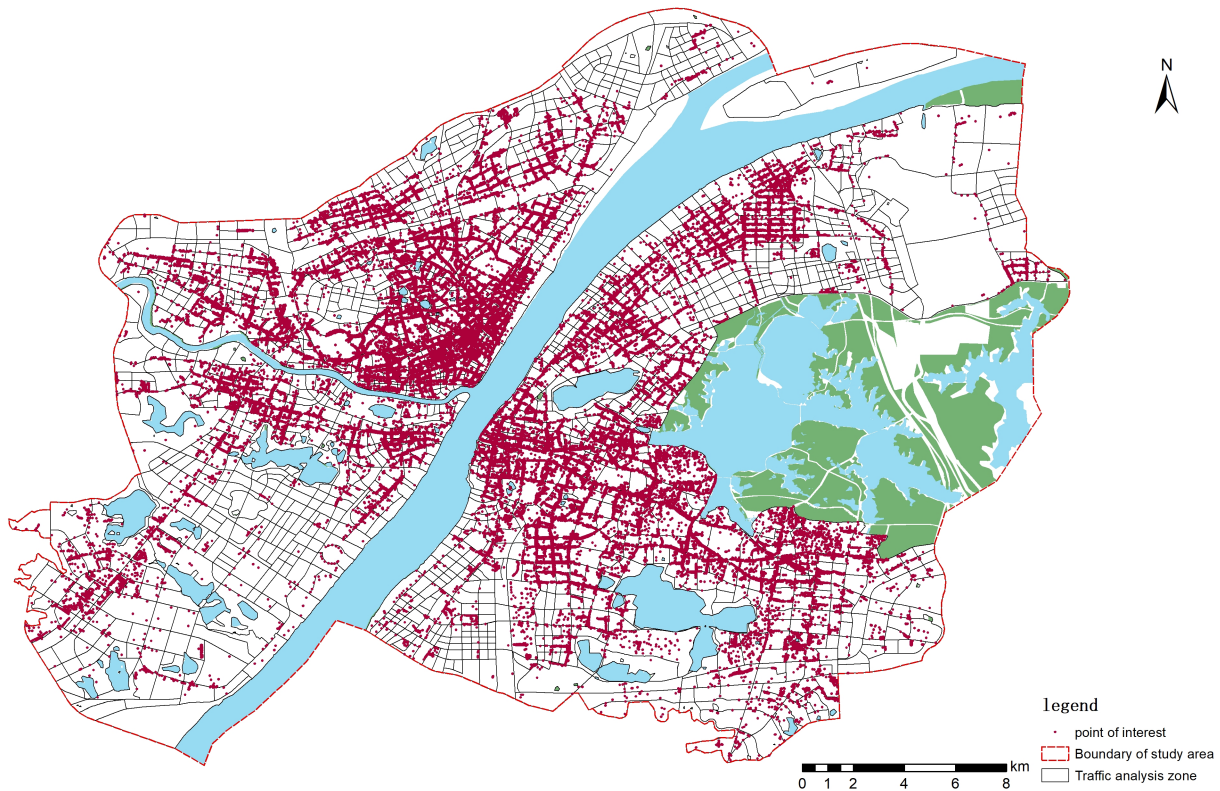


Figure 7. Spatial distribution of POIs.

3. Methods

3.1. Block Vitality Quantification

Block vitality can be expressed as the density of people performing activities in a unit spatial area. Compared with other data, the cellular signaling data can effectively reflect the real activity of people. Measuring block vitality by the distribution density of cellular signaling data has been proven to be effective [31,32].

$$V_i = X_i / S_i, \quad (1)$$

where V_i denotes the vitality of block i ($i = 1, 2 \dots M$, $M = 2395$); X_i denotes the number of people using mobile phones in block i during the study time period; and S_i represents the area of block i .

3.2. Indicator System Construction

Most of the existing studies examined its impact on block vitality in terms of a single aspect. Ying divided the influencing factors of block vitality into external and internal elements to consider the influencing elements of block vitality more systematically [44]. Environmental elements that influence block vitality were identified according to the existing research (Table 2) [3,5,50–52].

- (1) We used POI data representing the most fine-grained land uses to measure the function density of blocks and the degree of mixed functional use of blocks [5]. The spatial entropy of POIs was used to quantify the degree of mixed functional utilization of the block.
- (2) Green-looking ratio denotes the proportion of green plants in the scenery seen by people's eyes, which emphasizes the three-dimensional visual effect and represents a higher-level urban greening. The quantification of both green-looking ratio and sky view was attained by image segmentation of street-view images by machine learning.

Table 2. Indicator system.

Primary Indicator	Secondary Indicators	Unit
Block accessibility	C1 bus station density	pcs/km ²
	C2 distance of nearest subway station	Km
	C3 road density	Km/km ²
Block function	C4 function density	pcs/km ²
	C5 function-mixing degree	—
Block development intensity	C6 building density	—
	C7 floor area ratio	—
Block environment perception	C8 green-looking ratio	—
	C9 sky view	—

3.3. PSPNet Model Calculates the Percentage of Greenery and Sky in Street-View Images

PSPNet is a novel deep convolutional neural network model that classifies each pixel of an image and divides the image into several visually meaningful regions. Reportedly, it can be used to precisely and efficiently segment street-view images and identify the percentage of greenery, sky, and other elements [53–55]. The model schematic is shown in Figure 8. Based on a previous model, the model was trained using 1000 labeled images as the training set for machine learning to make the model more suitable for the research needs.

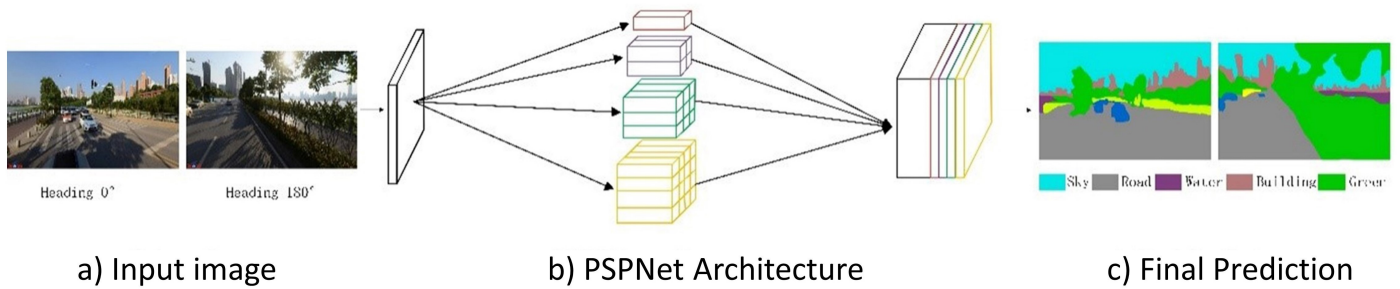


Figure 8. Schematic diagram of PSPNet model.

The image was segmented into five parts—building, sky, greenery, water, and road (Figure 9). The ratio of sky pixels to the total number of pixels in the image was calculated to represent the percentage of the sky in the image, and the green-looking ratio was calculated in the same way [55].

$$P_{i,sky\ enclosure} = P_{i,sky} \div N, \tag{2}$$

$$P_{i,greenery\ enclosure} = P_{i,greenery} \div N, \tag{3}$$

where $P_{i,sky}$, $P_{i,greenery}$ denote the number of pixels of sky and greenery; N denotes the total number of pixels of the image; and $P_{i,sky\ enclosure}$, $P_{i,greenery\ enclosure}$ denote the percentage of sky and greenery, respectively.

3.4. Spatial Entropy Calculation

Entropy is originally a physical concept used to measure the complexity and equilibrium of a system. The numerical magnitude of spatial entropy can reflect the degree of mixing of urban functions. The higher the entropy value, the more the functional types there are, the smaller the difference in the number of each functional type, and the higher the functional mix in this area.

$$P_i = T_i / A_i, \tag{4}$$

$$S_s = - \sum_i^M P_i \times \log P_i, \tag{5}$$

where T_i denotes the number of a certain type of POI in the i -th block; A_i denotes the total number of POIs in the i -th block ($i = 1, 2, 3 \dots M$); and S_s denotes the spatial entropy.

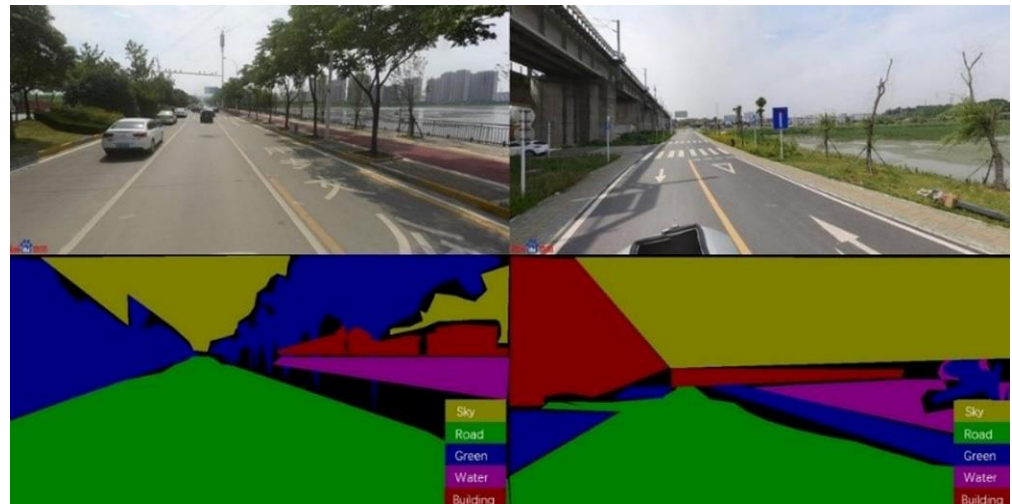


Figure 9. Schematic diagram of image segmentation results.

3.5. Geographically Weighted Regression

GWRs were used to explore the spatial heterogeneity of the impact of each indicator on block vitality. GWR was first presented in Brunson et al. [56]. In recent years, the model has been used widely in the field of urban planning to examine various elements of urban space. Compared with the ordinary linear regression model, GWR considers the existence of spatial heterogeneity. In addition, the model adds spatial coordinates as independent variables and imports spatial weight matrix to transform the regression region from global to local so that the model can reflect the spatial structural heterogeneity more realistically [57]. The GWR can be written as follows:

$$y_i = \beta_0 u_i, v_i + \sum_{t=1}^T x_{i,t} \beta_t(u_i, v_i) + \varepsilon_i, \quad (6)$$

where i denotes the number of blocks ($i = 1, 2 \dots M$); t is the number of features in the set $t = 1, 2 \dots T$; y_i is the vibrancy value of the i -th block; $x_{i,t}$ denotes the value of the t -th feature (explanatory variable) of the i -th observation; u_i, v_i are the geographic coordinates of the sampling points; $\beta_t(u_i, v_i)$ is the influence coefficient of the feature for a given geographic coordinate (GWR coefficient); ε_i is the error term.

4. Experiment and Result Analysis

4.1. Visualization of Environmental Elements and Spatial Distribution Patterns

4.1.1. Block Accessibility

Block accessibility comprises three elements—density of block road, density of block bus stations, and distance from the nearest subway station. The red color in Figure 10 represents high density and proximity, whereas the blue color denotes the opposite. As shown in Figure 10, the overall accessibility of the block exhibits a decreasing trend from the center to the outside. There were no evident high-value clusters of road density and bus station density. The distance to the subway station was distributed in strips along the rail line, and the Hankou district performed better in terms of distance to the subway station. Owing to the rapid growth and wide distribution of rail transit within the main urban area of Wuhan, most blocks are within 3 km of the subway station, except for a small number of blocks in the north and south of the study area.

4.1.2. Block Function

Block function comprises two components—block function density and block-function-mixing degree (Figure 11). The red color in Figure 11 represents high value. Both the function density and the functional mixing degree display the characteristics of high center and low surrounding; however, there is no apparent correlation between them. The north

side where the two rivers (Yangtze and Han) meet is the area with the highest density of POIs and the densest distribution of block functions, but this part of the block has single-type points of interest, implying a low-level block mixing and a single block function.

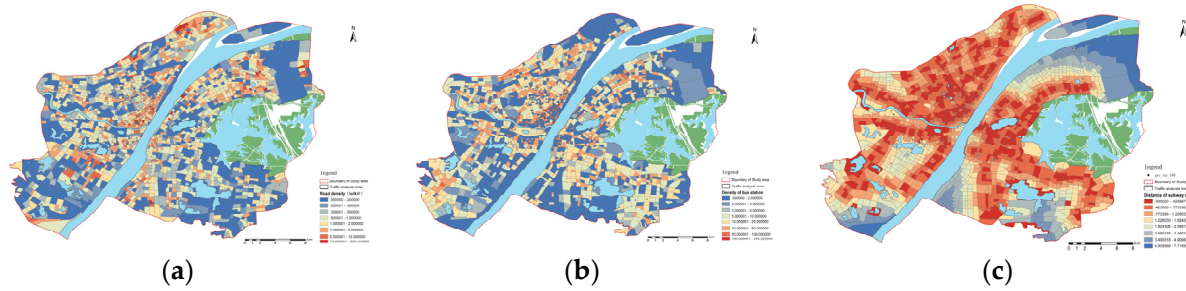


Figure 10. Neighborhood accessibility. (a) Road network density; (b) bus station density; (c) distance to the nearest subway station.

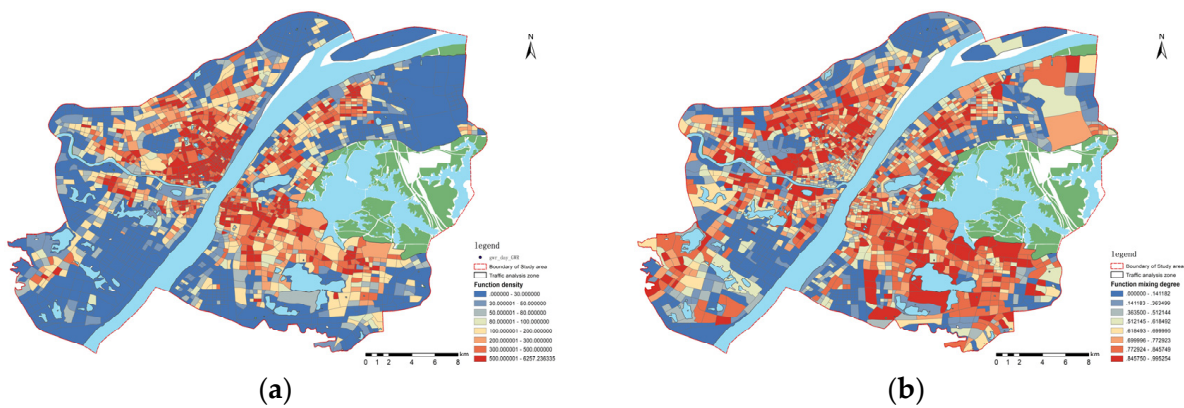


Figure 11. Block function. (a) Block function density; (b) block-function-mixing degree.

4.1.3. Block Development Intensity

Block construction intensity comprises floor area ratio and building density. Building density is a two-dimensional perspective that uses the building coverage of a parcel to quantify the development and utilization of flat land, whereas the floor area ratio considers the vertical development level of a block from a three-dimensional perspective (Figure 12). The graphs in Figure 12 are colored from red to blue to represent gradually decreasing values.

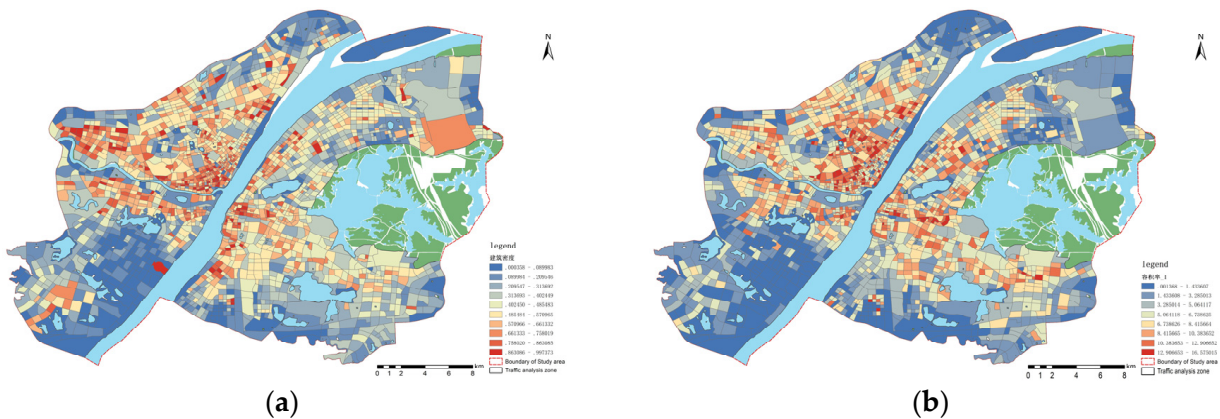


Figure 12. Block development intensity. (a) Building density; (b) floor area ratio.

The high values of building density and floor area ratio show a dotted distribution in Figure 12. The building density of the blocks west of the Yangtze River is marginally higher than that of the blocks east of the Yangtze River. The lack of control over building density during the construction of the old city of Hankou results in a high level of flat land development and utilization. Comparatively, the flat land development and utilization in Wuchang district are more balanced. The floor area ratio of buildings within the Third Ring Road is usually high, but that of blocks along the lake is low, especially around the East Lake; this correlates with the regulations associated with the skyline control around the lake issued by Wuhan in recent years. The building density of Zhuankou and Wugang area is high, but the plot ratio is very low, which closely correlates with the restricted height and low vertical construction of industrial park plants.

4.1.4. Block Environment Perception

In this study, the greenery and sky viewed from the human perspective were obtained and quantified using the PSPNet program to segment the Baidu Street View images. The mean value of the green-looking ratio of the sampled points within each block was used as the value of the block green-looking ratio index, and the sky visibility was obtained similarly (Figure 13). The color changes from red to blue in Figure 13 to represent a gradual decline in green-looking ratio and sky view.

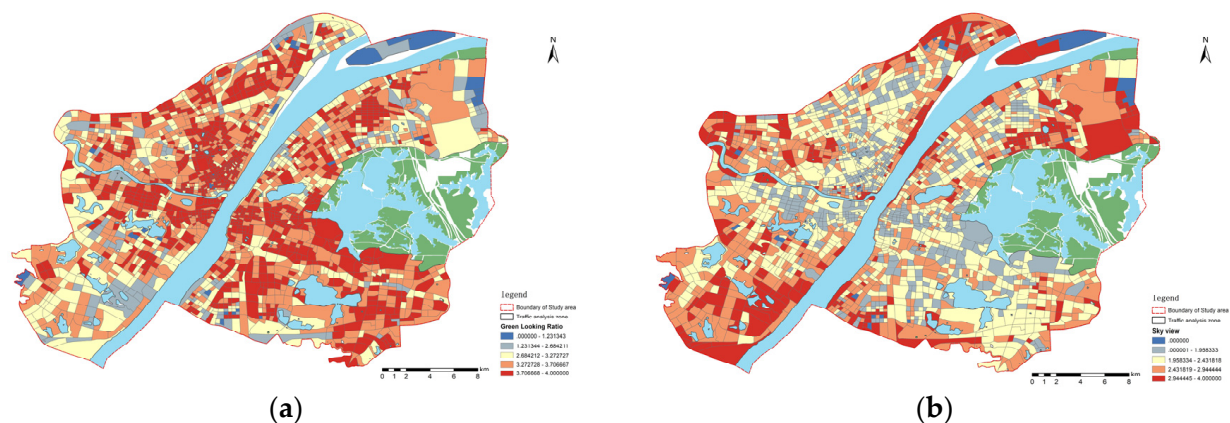


Figure 13. Block environment perception. (a) Green-looking ratio; (b) sky view.

From the color distribution of the two graphs, it is clear that a block with a high green-looking ratio has a lower sky view, which aligns with the general perception. A high green-looking ratio implies dense greenery, which can block people's view and decrease the percentage of visible sky. A small number of blocks have neither good greenery nor a wide view of the sky, which is caused by too little building spacing and too much building density. The block within the Third Ring Road of Wuhan city has good performance in green-looking ratio. Owing to the poor construction and the lack of attention to greening, the green-looking ratio of the blocks in the Zhuankou and Wugang areas is relatively poor. The blocks with a high sky view are concentrated in the vicinity of the Third Ring Road and the industrial parks outside the Third Ring Road. The visibility of the sky is low in the Luojia Mountain, Turtle Mountain, and East Lake Greenway areas where the greenery is excellent and in the old city of Hankou where the construction intensity is high.

4.2. Block Vitality Features

4.2.1. Distribution of Cellular Signaling Data

The collected cellular signaling data were organized by days and time periods (Figures 14–16). Figure 14 shows the total cellular signaling data for each day of the study period. Figure 15 shows the cellular signaling data for a week averaged in 1h units as a reflection of the prevailing situation for each hour of the week. The number of cell phone users is lowest from 3:00 to 5:00 throughout the day. From 7:00 onward, the number of cell phone users

starts snowballing. The number of people using cell phones reaches two peak values in a day during the dining hours of 11:00–12:00 and 17:00–18:00 but gradually decreases after 18:00. Figure 16 shows the distribution of cellular signaling data on average for workdays and weekends. Numerically, the number of people using cell phones from 23:00 to 5:00 on weekend nights is higher than that on workdays, reflecting that the city is more active on weekend nights.

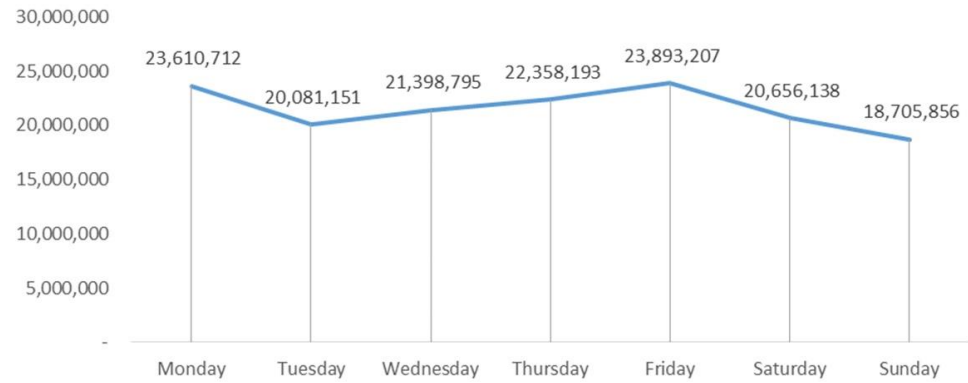


Figure 14. Cellular signaling data week distribution.

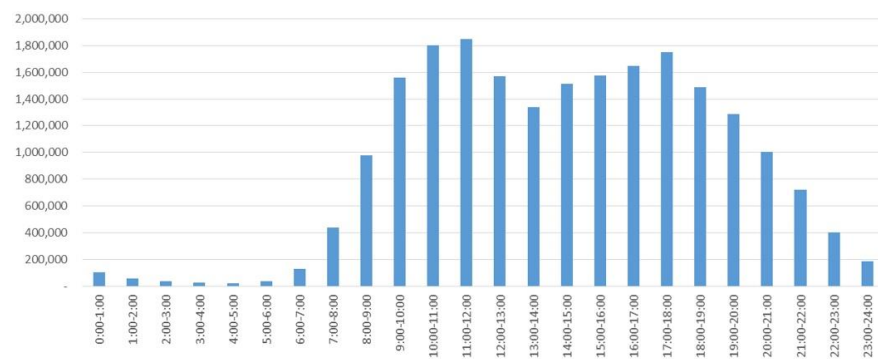


Figure 15. Hourly average distribution of cellular signaling data.

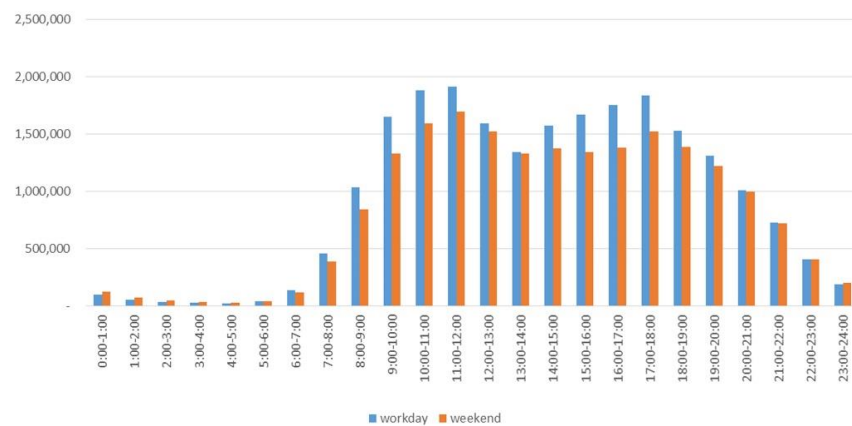


Figure 16. Comparison of hourly distribution of cellular signaling data between workdays and weekends.

4.2.2. Block Vitality Distribution

Figure 17 shows the spatial visualization of vitality. Block vitality forms a high-value agglomeration in southeastern Hankou and decays with increasing distance. The Wuchang area has created a major vibrant belt dominated by Yellow Crane Tower—Wuhan University—Huazhong University of Science and Technology. The Hanyang area forms a

vibrant belt distributed along the Hanshui. Both Zhuankou and Wugang are large industrial parks in Wuhan; however, the vitality value of Zhuankou area is marginally higher than that of Wugang area, which was built later and has better development momentum. The vitality of the residential area west of Wugang Avenue is significantly higher than that of the factory area on the east side.

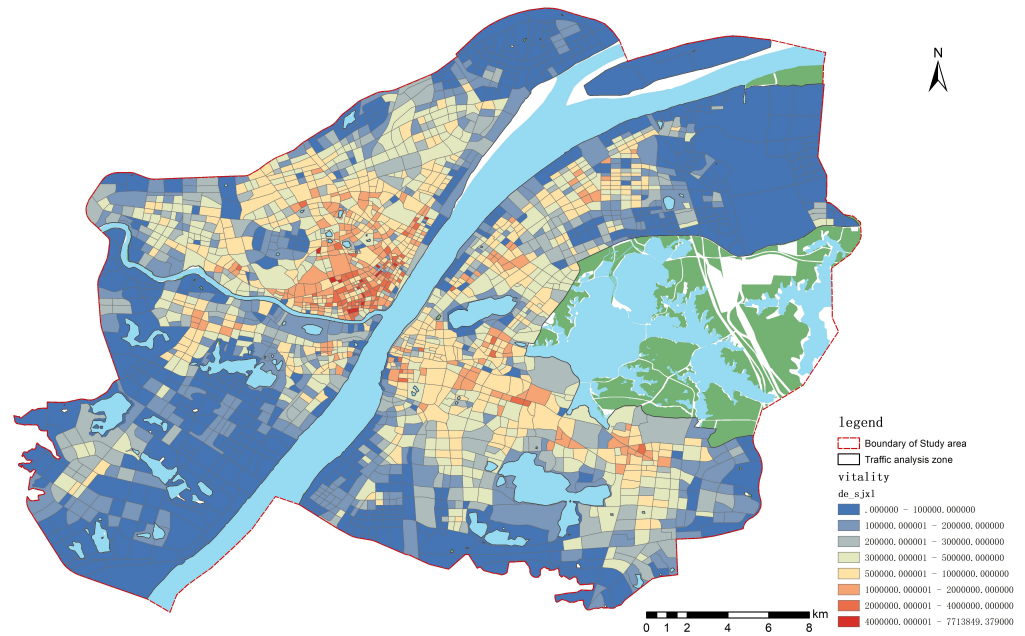


Figure 17. Block week vitality spatial distribution.

We visualized the average vitality of workdays versus weekends (Figure 18). The distribution of block vitality on workdays and weekends is closer. Compared with workdays, the distribution of block vitality on weekends is more balanced. The high-value aggregation area of Hankou’s vitality weakened significantly, and the vitality value of science, education, culture, and government office areas in Wuchang District decreased marginally over the weekends.

The vitality of workdays and weekends was categorized according to 4 h intervals (Figure 19). Consistent with the daily rhythm of human life, block vitality decreases significantly during nighttime, both workdays and weekends, and increases significantly from the morning peak at 8:00 until 20:00 when the vitality decreases significantly. The nighttime vitality is higher on weekends than on workdays, especially from 0:00 to 4:00. In addition, block vitality is higher during the daytime on workdays, especially in the Hankou business district and Wuchang Science Education Center.

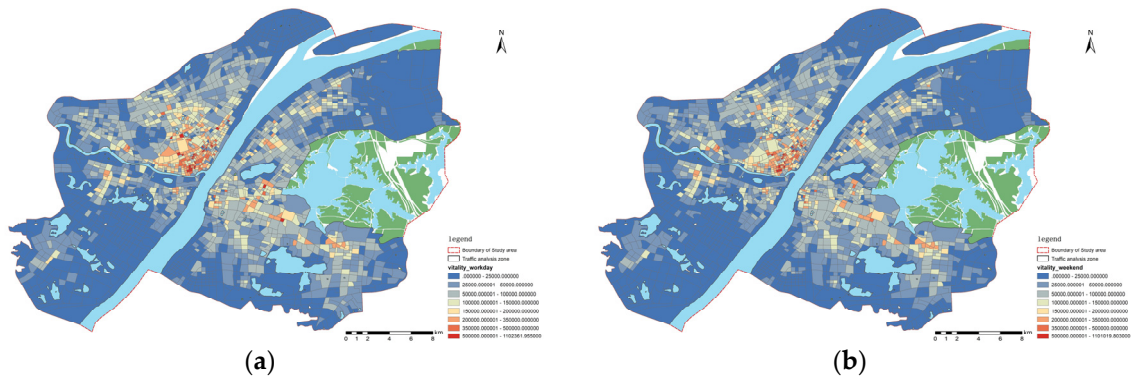


Figure 18. Comparison of the spatial distribution of block vitality. (a) Workday block vitality distribution; (b) weekend block vitality distribution.

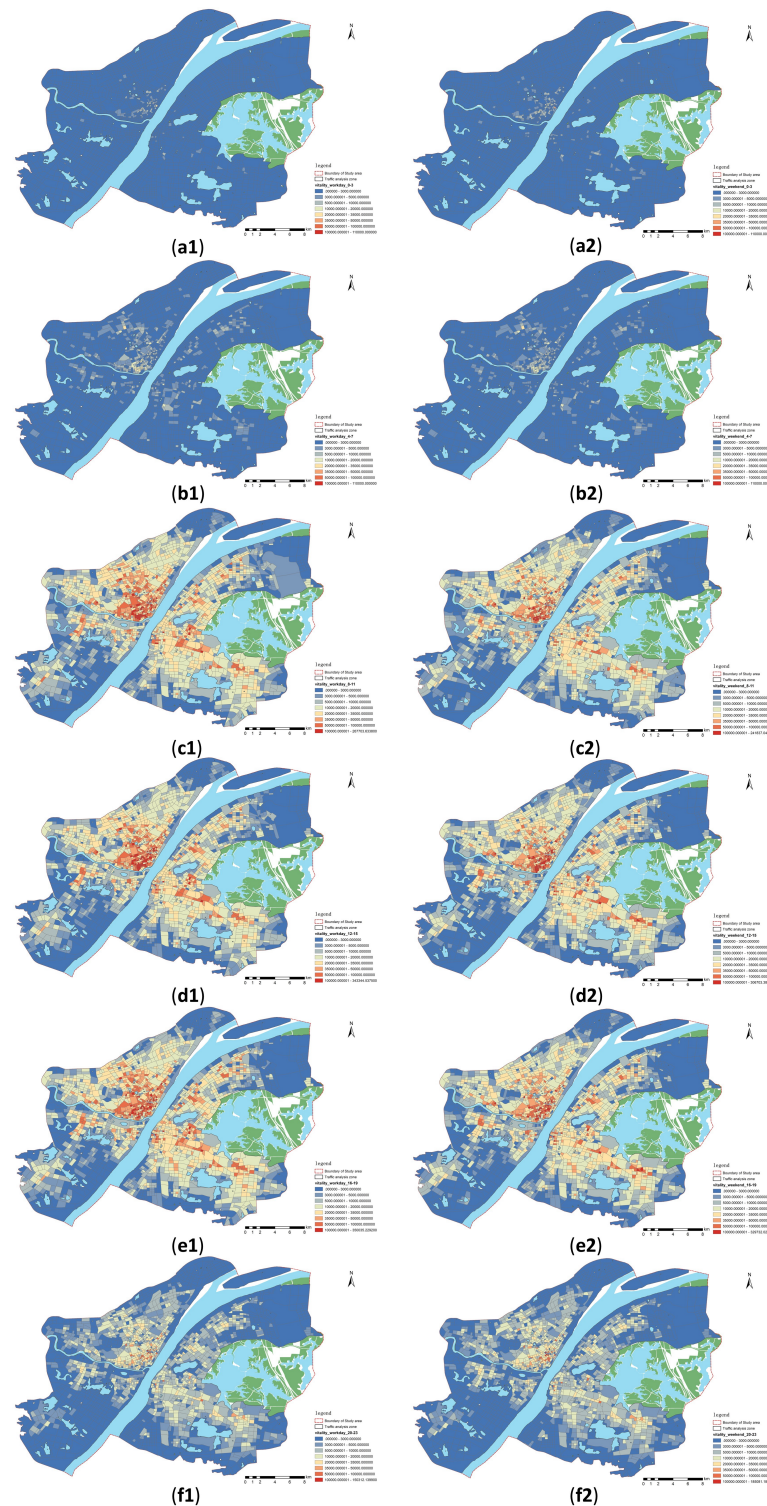


Figure 19. Comparison of block vitality by time period. (a1) Vitality distribution from 0:00 to 4:00 on workdays; (a2) vitality distribution from 0:00 to 4:00 on weekends; (b1) vitality distribution from 4:00 to 8:00 on workdays; (b2) vitality distribution from 4:00 to 8:00 on weekends; (c1) vitality distribution from 8:00 to 12:00 on workdays; (c2) vitality distribution from 8:00 to 12:00 on weekends; (d1) vitality distribution from 12:00 to 16:00 on workdays; (d2) vitality distribution from 12:00 to 16:00 on weekends; (e1) vitality distribution from 16:00 to 20:00 on workdays; (e2) vitality distribution from 16:00 to 20:00 on weekends; (f1) vitality distribution from 20:00 to 24:00 on workdays; (f2) vitality distribution from 20:00 to 24:00 on weekends.

4.3. Analysis of GWR Results

4.3.1. The Impact of Each Indicator on Block Vitality and Spatial Differentiation

We used the distribution density of the total value of cellular signaling data for a week as the dependent variable, and GWR was performed with the independent variable. To evade the problem of large differences in coefficients owing to the large differences in the indicators themselves, which are detrimental to the subsequent analysis, the independent variables were standardized so that the range of independent variables was uniformly controlled at [0, 1]. Tables 3 and 4 show the results. The adjusted R^2 value of 0.4328 indicates that the model's independent variables explain the dependent variable at a high level of 43.28% and the model fits well.

Table 3. GWR parameter table.

Varname	Variable
ResidualSquares	135.339448
EffectiveNumber	171.30417
Sigma	0.745226
AICc	1108.82647
R^2	0.666128
R^2 Adjusted	0.432804

Table 4. Regression coefficients of independent variables.

Independent Variable	Coefficient	Standard Deviation	VIF
C1 bus station density	0.717431	0.150015	1.128058
C2 distance of nearest subway station	−0.491072	0.080011	1.148059
C3 road density	1.282304	0.207124	1.103493
C4 function density	3.594345	0.155446	1.341426
C5 function-mixing degree	0.076683	0.077442	1.496915
C6 building density	0.239677	0.040434	1.939019
C7 floor area ratio	0.181675	0.062733	2.315423
C8 green-looking ratio	0.045766	0.082143	1.251804
C9 sky view	−0.108025	0.071294	1.147594

The VIF of each independent variable is <7.5, which identifies the absence of multicollinearity between the indicators in Table 3. The coefficients effectively reflect the positive and negative impact of each indicator on block vitality and the magnitude of the impact. According to Table 3, the distance from the nearest subway station and sky view negatively correlated with block vitality, that is, the further the distance from the subway station and the higher the sky view, the lower the block vitality value. In addition, block function density and road density exert a high degree of influence on block vitality and the influence of block-function-mixing degree and green-looking ratio on block vitality is relatively small.

One of the differences between GWR and other regression methods is that GWR can calculate impact coefficients for each indicator in each region. We visualized the coefficients of each indicator for each block (Figure 20). The blue area in Figure 20 represents high-intensity negative impact, the red area represents high-intensity positive impact, and the yellow area is low impact; the effect of each indicator on block vitality is spatially nonhomogeneous and varies extensively.

At the block accessibility level, bus station density exerts a significant positive impact on the vitality of the predominantly industrial-attributed blocks around Wuhan's Third Ring Road. Negative impact areas for the bus station density occur around the Second Ring Road and the Beijing–Guangzhou Railway. The blocks in these negative impact areas have higher bus station densities; therefore, the negative impacts, such as traffic congestion due to bus stations, outweigh the positive impacts on the vitality of these blocks. The impact of distance to the nearest subway station on the vitality of most blocks is negative, with only

a few blocks having a very low positive effect. The impact of this indicator on block vitality did not exhibit significant polarization. The distribution of the effect of road density on block vitality is relatively homogeneous, with few blocks having both strong positive and negative correlations. In addition, block accessibility has a strong positive correlation with the vitality of science, education, and culture places, such as university cities and high-tech parks, which is effectively verified at three levels—bus station density, distance to the nearest subway station, and road network density. This finding suggests that enhancing block vitality with a predominantly cultural and educational land-use nature could start with enhancing the block accessibility.

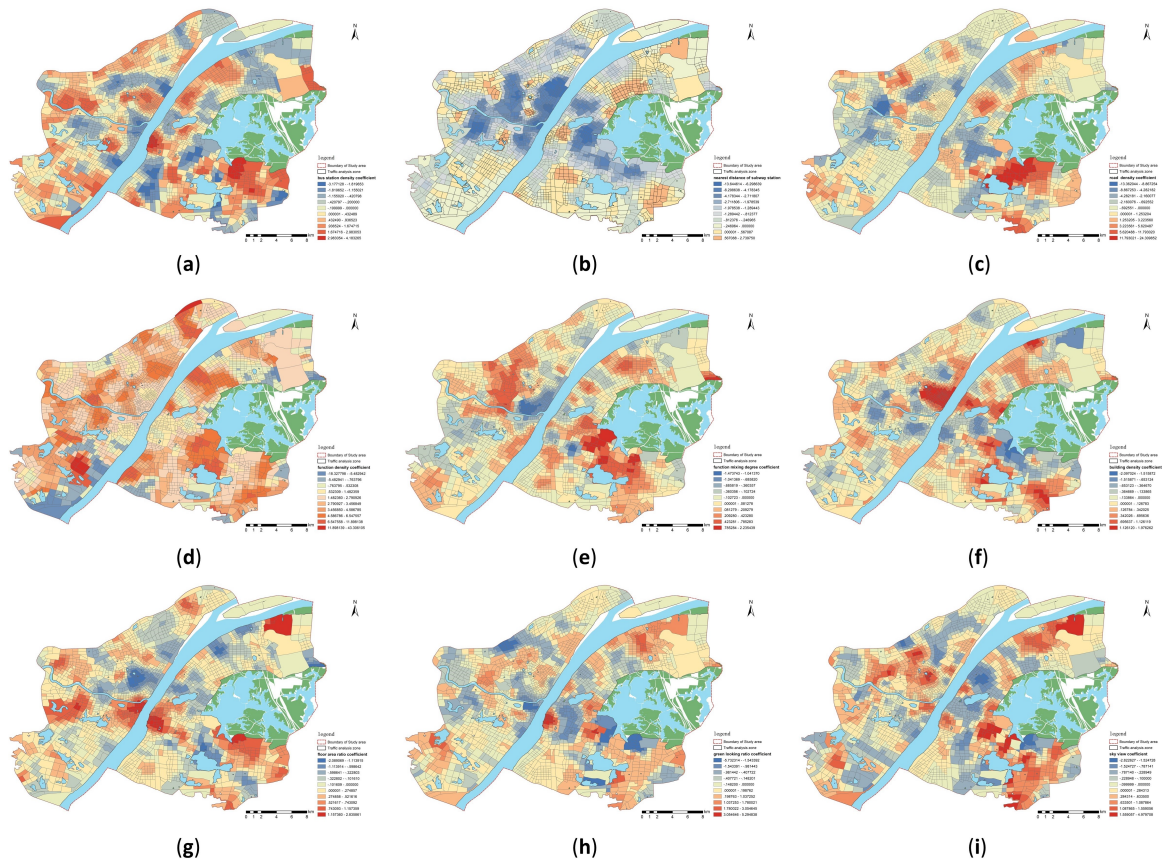


Figure 20. Distribution of regression coefficients of each indicator. (a–i) represent the influence coefficients of each indicator.

The block function density exerts a greater impact on block vitality than the degree of function mixing in a block. In addition, the block function density exerts a positive impact on the vitality, that is, the higher the function density, the stronger the ability to attract residents' activities and the greater the intensity of block vitality. The function-mixing degree of a block can effectively reflect the degree of diversity of land use. For the residential-oriented blocks in central Hankou and the blocks in the university area of Wuchang District, the block-function-mixing degree exerts a significant positive impact on block vitality. However, in the case of the old city of Hankou, where the block functions are already highly compounded, this indicator no longer exerts a significant positive effect. Of note, blocks with a single land-use function can be quickly enhanced by increasing the functional mix of the blocks.

The two indicators of building density and floor area ratio are combined to reflect the impact of the degree of block construction on block vitality, and the combined impact value of both indicators is positive. Combining Figure 20f,g shows that the vitality of the peripheral blocks in the main urban area of Wuhan is positively affected by the building density and floor area ratio. In addition, the mechanism of the effect of building density

and building volume ratio in some blocks in the center of the main urban area is completely opposite. The blocks in the Turtle Mountain Scenic Area and the University City area of Wuchang District can be effectively improved by decreasing the building density and increasing the plot ratio to enhance the vitality.

Beautiful greenery and suitable sky openness regulate the block climate and encourage people to travel. The vitality of industrial areas in different zones inside and outside the Third Ring Road responds to the opposite degree of the green-looking ratio. Zhuankou and Wugang are located outside the Third Ring Road of the city, which is derailed from the city center. The low local emphasis on block greening leads to a more attractive block with a high green-looking ratio; thus, increasing the green-looking ratio of the two industrial parks can effectively encourage people's travel behavior and enhance block vitality. Turtle Mountain Scenic Area and the southern part of East Lake have reached saturation with the positive effect of the green-looking ratio on people's travel owing to the government's attention and excellent native natural conditions. By appropriately pruning street trees, decreasing building heights, and improving building spacing, the spatial openness can be enhanced to promote human stay activities.

4.3.2. The Impact of Each Indicator on Block Vitality Based on Workdays and Weekends

To compare the variability of the impact of each indicator on block vitality between weekends and workdays, the cellular signaling data from Monday to Friday were averaged to evaluate the distribution density as the block vitality of workdays and the vitality of weekends were calculated similarly. To circumvent the differences in the impact coefficients of the indicators owing to the differences in vitality on workdays and weekends, the block vitality on workdays and weekends was normalized and then subjected to GWR with the indicators. Tables 5 and 6 show the results.

Table 5. Comparison of the degree of explanation.

	Workday	Weekend
R ²	0.665935	0.662769
R ² Adjusted	0.432477	0.427099

Table 6. Comparison of regression coefficients.

Independent Variable	Workday		Weekend	
	Coefficient	VIF	Coefficient	VIF
C1 bus station density	0.095924	1.128058	0.0857	1.128058
C2 distance of nearest subway station	−0.067445	1.148059	−0.05419	1.148059
C3 road density	0.172378	1.103493	0.150854	1.103493
C4 function density	0.474224	1.341426	0.445276	1.341426
C5 function-mixing degree	0.011078	1.496915	0.007094	1.496915
C6 building density	0.031165	1.939019	0.030836	1.939019
C7 floor area ratio	0.027007	2.315423	0.014903	2.315423
C8 green-looking ratio	0.006381	1.251804	0.004810	1.251804
C9 sky view	−0.013195	1.147594	−0.016030	1.147594

No covariance occurred among all indicators of the two models. The degree of explanation of the independent variables on the changes of the dependent variable in the two models was 43.25% and 42.71%. Only one indicator, sky visibility, exerted a greater impact on block vitality on weekends than on workdays.

To visually compare the differences of each indicator on block vitality enhancement on workdays and weekends, let R_{i1} represent the coefficient of the R indicator of block i on workdays and R_{i2} denote the coefficient of the R indicator of block i on weekends. There are six cases to calculate the $R_{i1} - R_{i2}$ difference (Table 7).

Table 7. Situation and meaning.

R_{i1}	R_{i2}	$R_{i1} - R_{i2}$	Meaning
+	+	+	The increase in vitality on weekends for this indicator is higher than on workdays.
+	+	-	The increase in vitality on weekends for this indicator is lower than on workdays.
-	-	+	The increase in vitality on weekends for this indicator is higher than on workdays.
-	-	-	The increase in vitality on weekends for this indicator is lower than on workdays.
+	-	+	The increase in vitality on weekends for this indicator is higher than on workdays.
-	+	-	The increase in vitality on weekends for this indicator is lower than on workdays.

Figure 21 shows the spatial visualization of the differences in the impact coefficients of each indicator; red denotes a positive difference, implying that the block has a greater boost to vitality on weekends than on workdays for this indicator, and vice versa in blue, while yellow represents the extent to which this indicator affects block vitality independently of workdays or weekends.

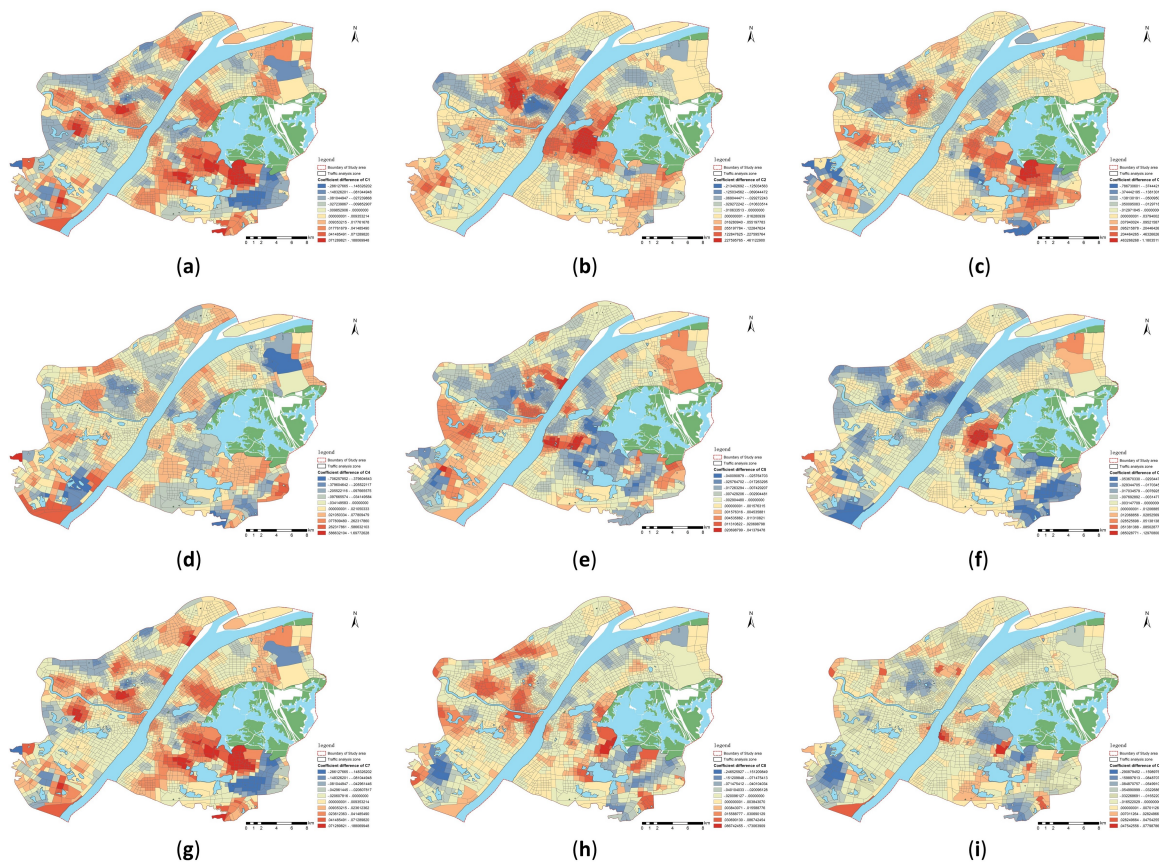


Figure 21. Spatial distribution of regression coefficient differences. (a–i) represent the regression coefficient differences of each indicator.

Comparing the three indicators of accessibility, the effect of bus station density is higher than the other two indicators by time period. The positive impact of accessibility in the south of the East Lake is higher on weekends than on workdays. The southern part of East Lake is the center of education in Wuhan, where numerous college students gather. College students have a higher demand for going out on weekends, and the enhancement

of block accessibility on weekends exerts a significant impact on enhancing block vitality. Comparing the two indicators of block function, the function density and function-mixing degree exert a significant effect on enhancing the vitality in Zhuankou on weekends. In addition, Zhuankou Industrial Park is characterized by short construction time, low degree of perfection of supporting facilities, and single nature of land use. With workers seeking a higher quality of recreational life on their days off, high-density and high-mix blocks exert a more pronounced effect on attracting foot traffic. Compared with other indicators, the impact of human perception of block environment is less influenced by the time of day, especially the indicator of sky view.

Generally, the enhancement of block vitality by each indicator closely correlates with whether elements such as the main functions, current conditions, and needs of the block are influenced by weekdays versus weekends.

5. Conclusions and Discussion

Now is an era of rapid development of big data; cellular signaling data as a type of big data can effectively reflect the spatial and temporal characteristics of human behavior. This study used the distribution density of cellular signaling data to quantify block vitality and constructed an index system for the block environment. In addition, human perception of the environment was introduced into the index system. Streetscape image segmentation was used to attain the perception of greenery and sky to better fit the human perspective. Finally, GWR was used to reflect the temporal and spatial impact mechanism of the indicator on the vitality of the block, and according to the impact mechanism, it contributed to making reasonable suggestions for improving block vitality. The following conclusions were drawn from this study:

First, block vitality has significant spatial and temporal heterogeneity. Overall, vitality is stronger and more concentrated in downtowns than in distant urban areas. Block vitality is at its lowest in the early hours of the day and peaks during lunch and dinnertime. Block vitality on weekends is more balanced with a decrease in the peak. Nighttime vitality on weekends is higher than on workdays.

Second, indicators of block environment have large variability in their impact on block vitality. The most influential indicators are the function density of the block and the road density, whereas the less influential indicators are the function-mixing degree and the sky view. Enhancing the accessibility of blocks can be done by increasing the density of bus stations, rationalizing subway lines to decrease the distance from the nearest subway station, and implementing a “small block and dense road network.” Facilitating people’s travel behavior is a necessary condition for the growth of block vitality. Increasing building density and floor area ratio in poorly built-up areas can accommodate more social behavior to attain block vitality growth. Increasing the function density and mix of functions in a block can attract more people to work, live, relax, and play. By increasing the block attractiveness, the vitality can be increased. Finally, beautiful greenery, shade, and open views will attract people to go out and promote block vitality, especially in blocks with poorly constructed existing greenery.

Finally, a gap exists between the impact of each indicator on workdays and weekends. Owing to the differences in the behavioral characteristics of people on workdays and weekends, the degree of influence of each indicator on block vitality also varies. For example, for blocks with a high demand for weekend outings, such as universities, improving block accessibility can effectively enhance block vitality. Blocks with a single function, such as industrial parks, can be made more vibrant by increasing the functional density and functional mix of the block.

6. Contributions and Limitations

People are paying increasing attention to the human living environment in recent years. As a crucial index to measure the degree of urban development and enhance the human living environment, the study of its quantification and influencing factors is

essential to improve block vitality. This study intended to enrich the quantitative form of block vitality and improve the index system of block vitality by examining the influencing factors and mechanisms of block vitality in Wuhan and, meanwhile, hopes that the findings will provide reference suggestions for the enhancement of block vitality in other cities.

From a theoretical perspective, the innovation points of this study are primarily reflected in the following two points. First, this study used cellular signaling data that reflect the spatial and temporal characteristics of human behavior. Cellular signaling data have the advantages of a large sample size and reliable information, which can completely reflect the real condition of workdays and weekends compared with traditional data. Second, this study added human perception of the environment to the index system of block vitality evaluation. Using streetscape image segmentation to quantify the green-looking ratio and openness of the block from a human perspective fills the gap of human perception of the environment in block vitality research and reflects the human-centered planning idea. From a practical perspective, this study focused on dynamic block vitality and examined ways to enhance block vitality by dividing it into workdays and weekends, as opposed to previous studies of static vitality.

Although this study has many advantages, some limitations need to be addressed subsequently. First, with respect to the dependent variable, the activities of some people who do not engage in mobile communication behaviors were overlooked when quantifying block vitality. Subsequent studies can combine other indicators to jointly enhance the quantification of block vitality. Second, in terms of environmental elements, the environmental elements in this study considered more physical environmental elements, while social environmental elements such as population size and economic development were not included in the consideration [58]. Green-looking ratio and openness as human perception of the environment were included in this study, but human perception of emotion is diverse, and other elements such as human emotions in different environments should also be included in the index system in subsequent studies to more comprehensively consider the impact of human perception on block vitality.

Author Contributions: Conceptualization, H.J.; methodology, H.J. and Y.Y.; software, Y.Y.; validation, H.J., Y.Y. and Y.M.; formal analysis, Y.Y.; investigation, H.J.; resources, H.J.; data curation, Y.Y. and Y.M.; writing—original draft preparation, Y.Y.; writing—review and editing, H.J. and Y.M.; visualization, Y.Y. and Y.M.; supervision, H.J.; project administration, H.J.; funding acquisition, H.J. All authors have read and agreed to the published version of the manuscript.

Funding: This research was funded by the National Key Research and Development Program “Research and Development of Emergency Response and Collaborative Command System with Holographic Perception of Traffic Network Disaster” (2020YFC1512002).

Data Availability Statement: Not applicable.

Conflicts of Interest: The authors declare no conflict of interest.

References

- Jacobs, J.M.; Smith, S.J. Living room: Rematerialising home. *Environ. Plan. A* **2008**, *40*, 515–519. [[CrossRef](#)]
- Guo, X.; Chen, H.; Yang, X. An evaluation of street dynamic vitality and its influential factors based on multi-source big data. *ISPRS Int. J. Geo-Inf.* **2021**, *10*, 143. [[CrossRef](#)]
- Lu, S.; Huang, Y.; Shi, C.; Yang, X. Exploring the associations between urban form and neighborhood vibrancy: A case study of Chengdu, China. *ISPRS Int. J. Geo-Inf.* **2019**, *8*, 165. [[CrossRef](#)]
- Chhetri, P.; Stimson, R.J.; Western, J. Modelling the factors of neighbourhood attractiveness reflected in residential location decision choices. *Stud. Reg. Sci.* **2006**, *36*, 393–417. [[CrossRef](#)]
- Yue, Y.; Zhuang, Y.; Yeh, A.G.O.; Xie, J.Y.; Ma, C.L.; Li, Q.Q. Measurements of POI-based mixed use and their relationships with neighbourhood vibrancy. *Int. J. Geogr. Inf. Sci.* **2016**, *31*, 658–675. [[CrossRef](#)]
- Medved, P. The essence of neighbourhood community centres (NCCs) in European sustainable neighbourhoods. *Urban Des. Int.* **2017**, *22*, 150–167. [[CrossRef](#)]
- Malizia, E.; Motoyama, Y. The economic development–vibrant center connection: Tracking high-growth firms in the DC region. *Prof. Geogr.* **2015**, *68*, 349–355. [[CrossRef](#)]

8. Braun, L.M.; Malizia, E. Downtown vibrancy influences public health and safety outcomes in urban counties. *J. Transp. Health* **2015**, *2*, 540–548. [[CrossRef](#)]
9. Dave, S. Neighbourhood density and social sustainability in cities of developing countries. *Sustain. Dev.* **2011**, *19*, 189–205. [[CrossRef](#)]
10. Ewing, R.; Cervero, R. Travel and the built environment: A meta-analysis. *J. Am. Plan. Assoc.* **2010**, *76*, 265–294. [[CrossRef](#)]
11. Jalaladdini, S.; Oktay, D. Urban public spaces and vitality: A socio-spatial analysis in the streets of Cypriot towns. *Procedia Soc. Behav. Sci.* **2012**, *35*, 664–674. [[CrossRef](#)]
12. Montgomery, J. Making a city: Urbanity, vitality and urban design. *J. Urban Des.* **2007**, *3*, 93–116. [[CrossRef](#)]
13. Katz, P. *New Urbanism: Towards an Architecture of Community*; McGraw-Hill Education: New York, NY, USA, 1993.
14. Gehl, J. *Life between Buildings: Using Public Space*; Island Press: Washington, DC, USA, 1987.
15. Sung, H.; Lee, S.; Cheon, S. Operationalizing Jane Jacobs’s urban design theory: Empirical verification from the great city of Seoul, Korea. *J. Plan. Educ. Res.* **2015**, *35*, 117–130. [[CrossRef](#)]
16. Van Nes, A. Typology of Shopping Areas in Amsterdam. In Proceedings of the Space Syntax. 5th International Symposium, TU Delft, Amsterdam, The Netherlands, 13–17 June 2005.
17. Joosten, V.; Van Nes, A. How block types influences the natural movement economic process: Micro-spatial conditions on the dispersal of shops and Café in Berlin. In Proceedings of the 5th International Space Syntax Symposium, TU Delft, Delft, The Netherlands, 13–17 June 2005.
18. Levin, N.; Duke, Y. High spatial resolution night-time light images for demographic and socio-economic studies. *Remote Sens. Environ.* **2012**, *119*, 1–10. [[CrossRef](#)]
19. Levin, N.; Zhang, Q. A global analysis of factors controlling VIIRS nighttime light levels from densely populated areas. *Remote Sens. Environ.* **2017**, *190*, 366–382. [[CrossRef](#)]
20. Xia, C.; Yeh, A.G.O.; Zhang, A. Analyzing spatial relationships between urban land use intensity and urban vitality at street block level: A case study of five Chinese megacities. *Landsc. Urban. Plan.* **2020**, *193*, 103669. [[CrossRef](#)]
21. Babu, D.; Anjaneyulu, M.V.L.R. Exploratory analysis on worker’s independent and joint travel patterns during weekdays and weekends. *Transp. Eng.* **2021**, *5*, 100073. [[CrossRef](#)]
22. Gao, J.; Kamphuis, C.B.M.; Helbich, M.; Ettema, D. What is ‘neighborhood walkability’? How the built environment differently correlates with walking for different purposes and with walking on weekdays and weekends. *J. Transp. Geogr.* **2020**, *88*, 102860. [[CrossRef](#)]
23. Ye, Y.; Van Nes, A. Measuring urban maturation processes in Dutch and Chinese new towns: Combining street network configuration with building density and degree of land use diversification through GIS. *J. Space Syntax* **2013**, *4*, 18–37.
24. Banerjee, T. The future of public space: Beyond invented streets and reinvented places. *J. Am. Plan. Assoc.* **2001**, *67*, 9–24. [[CrossRef](#)]
25. Ye, Y.; Li, D.; Liu, X. How block density and typology affect urban vitality: An exploratory analysis in Shenzhen, China. *Urban. Geogr.* **2017**, *39*, 631–652. [[CrossRef](#)]
26. Sung, H.; Lee, S. Residential built environment and walking activity: Empirical evidence of Jane Jacobs’ urban vitality. *Transp. Res. D Transp. Environ.* **2015**, *41*, 318–329. [[CrossRef](#)]
27. Wasfi, R.A.; Dasgupta, K.; Eluru, N.; Ross, N.A. Exposure to walkable neighbourhoods in urban areas increases utilitarian walking: Longitudinal study of Canadians. *J. Transp. Health* **2016**, *3*, 440–447. [[CrossRef](#)]
28. Ratti, C.; Frenchman, D.; Pulselli, R.M.; Williams, S. Mobile Landscapes: Using location data from cell phones for urban analysis. *Environ. Plan. B Plan. Des.* **2006**, *33*, 727–748. [[CrossRef](#)]
29. Jacobs-Crisioni, C.; Rietveld, P.; Koomen, E.; Tranos, E. Evaluating the Impact of Land-Use Density and Mix on Spatiotemporal Urban Activity Patterns: An Exploratory Study Using Mobile Phone Data. *Environ. Plan. A Econ. Space* **2014**, *46*, 2769–2785. [[CrossRef](#)]
30. Wu, W.; Niu, X. Influence of Built Environment on Urban Vitality: Case Study of Shanghai Using Mobile Phone Location Data. *J. Urban Plan. Dev.* **2019**, *145*, 04019007. [[CrossRef](#)]
31. Candia, J.; González, M.C.; Wang, P.; Schoenharl, T.; Madey, G.; Barabási, A.L. Uncovering individual and collective human dynamics from mobile phone records. *J. Phys. A Math. Theor.* **2008**, *41*, 224015. [[CrossRef](#)]
32. Shi, L.; Chi, G.; Liu, X.; Liu, Y. Human mobility patterns in different communities: A mobile phone data-based social network approach. *Ann. GIS* **2015**, *21*, 15–26. [[CrossRef](#)]
33. Chen, X.; Kanna, A. *Rethinking Global Urbanism: Comparative Insights from Secondary Cities*; Routledge: London, UK, 2012.
34. Burgess, R.; Jenks, M. *Compact Cities: Sustainable Urban. Forms for Developing Countries*; Routledge: London, UK, 2000.
35. Liu, X.; Long, Y. Automated identification and characterization of parcels with OpenStreetMap and points of interest. *Environ. Plan. B Plan. Des.* **2016**, *43*, 341–360. [[CrossRef](#)]
36. Wu, C.; Ye, X.; Ren, F.; Du, Q. Check-in behaviour and spatio-temporal vibrancy: An exploratory analysis in Shenzhen, China. *Cities* **2018**, *77*, 104–116. [[CrossRef](#)]
37. Sarkar, C.; Webster, C.; Pryor, M.; Tang, D.; Melbourne, S.; Zhang, X.; Liu, J. Exploring associations between urban green, street design and walking: Results from the Greater London boroughs. *Landsc. Urban. Plan.* **2015**, *143*, 112–125. [[CrossRef](#)]
38. Liu, Y.; Liu, X.; Gao, S.; Gong, L.; Kang, C.; Zhi, Y.; Chi, G.; Shi, L. Social sensing: A new approach to understanding our socioeconomic environments. *Ann. Am. Assoc. Geogr.* **2015**, *105*, 512–530. [[CrossRef](#)]

39. Xia, Y.; Yabuki, N.; Fukuda, T. Development of a system for assessing the quality of urban street-level greenery using street view images and deep learning. *Urban For. Urban Green.* **2021**, *59*, 126995. [[CrossRef](#)]
40. Yue, W.; Chen, Y.; Thy, P.T.M.; Fan, P.; Liu, Y.; Zhang, W. Identifying urban vitality in metropolitan areas of developing countries from a comparative perspective: Ho Chi Minh City versus Shanghai. *Sustain. Cities Soc.* **2021**, *65*, 102609. [[CrossRef](#)]
41. Lu, S.; Shi, C.; Yang, X. Impacts of Built Environment on Urban Vitality: Regression Analyses of Beijing and Chengdu, China. *Int. J. Environ. Res. Public Health* **2019**, *16*, 4592. [[CrossRef](#)]
42. Liu, M.; Jiang, Y.; He, J. Quantitative evaluation on street vitality: A case study of Zhoujiadu community in Shanghai. *Sustainability* **2021**, *13*, 3027. [[CrossRef](#)]
43. Wu, H.L.; Cheng, W.C.; Shen, S.L.; Lin, M.Y.; Arulrajah, A. Variation of hydro-environment during past four decades with underground sponge city planning to control flash floods in Wuhan, China: An overview. *Undergr. Space* **2020**, *5*, 184–198. [[CrossRef](#)]
44. Kang, J.; Körner, M.; Wang, Y.; Taubenboeck, H.; Zhu, X.X. Building instance classification using street view images. *ISPRS J. Photogramm. Remote Sens.* **2018**, *145*, 44–59. [[CrossRef](#)]
45. Klimek, R. Towards recognising individual behaviours from pervasive mobile datasets in urban spaces. *Sustainability* **2019**, *11*, 1563. [[CrossRef](#)]
46. Chen, Y.; Zhang, Z.; Liang, T. Assessing urban travel patterns: An analysis of traffic analysis zone-based mobility patterns. *Sustainability* **2019**, *11*, 5452. [[CrossRef](#)]
47. Li, J.; Ye, Q.; Deng, X.; Liu, Y.; Liu, Y. Spatial-temporal analysis on spring festival travel rush in China based on multisource big data. *Sustainability* **2016**, *8*, 1184. [[CrossRef](#)]
48. Zhang, F.; Zu, J.; Hu, M.; Zhu, D.; Kang, Y.; Gao, S.; Zhang, Y.; Huang, Z. Uncovering inconspicuous places using social media check-ins and street view images. *Comput. Environ. Urban Syst.* **2020**, *81*, 101478. [[CrossRef](#)]
49. Zeng, L.; Lu, J.; Li, W.; Li, Y. A fast approach for large-scale Sky View Factor estimation using street view images. *Build. Environ.* **2018**, *135*, 74–84. [[CrossRef](#)]
50. Long, Y. Street urbanism a new perspective for urban studies and city planning in the new data environment. *Time Archit.* **2016**, 128–132. (In Chinese) [[CrossRef](#)]
51. Winters, M.; Brauer, M.; Setton, E.M.; Teschke, K. Built environment influences on healthy transportation choices: Bicycling versus driving. *J. Urban Health* **2010**, *87*, 969–993. [[CrossRef](#)]
52. Delafons, J. The New Urbanism: Toward an Architecture of Community: Peter Katz. *Cities* **1994**, *11*, 342–343. [[CrossRef](#)]
53. Gong, Z.; Ma, Q.; Kan, C.; Qi, Q. Classifying street spaces with street view images for a spatial indicator of urban functions. *Sustainability* **2019**, *11*, 6424. [[CrossRef](#)]
54. Chen, X.; Meng, Q.; Hu, D.; Zhang, L.; Yang, J. Evaluating greenery around streets using Baidu panoramic street view images and the panoramic green view index. *Forests* **2019**, *10*, 1109. [[CrossRef](#)]
55. Hu, F.; Liu, W.; Lu, J.; Song, C.; Meng, Y.; Wang, J.; Xing, H. Urban function as a new perspective for adaptive street quality assessment. *Sustainability* **2020**, *12*, 1296. [[CrossRef](#)]
56. Brunson, C.; Fotheringham, A.S.; Charlton, M.E. Geographically weighted regression: A method for exploring spatial nonstationarity. *Geogr. Anal.* **1996**, *28*, 281–298. [[CrossRef](#)]
57. Kopczewska, K.; Cwiakowski, P. Spatio-temporal stability of housing submarkets. Tracking spatial location of clusters of geographically weighted regression estimates of price determinants. *Land Use Policy* **2021**, *103*, 105292. [[CrossRef](#)]
58. Mouratidis, K.; Poortinga, W. Built environment, urban vitality and social cohesion: Do vibrant neighborhoods foster strong communities? *Landsc. Urban Plan.* **2020**, *204*, 103951. [[CrossRef](#)]